Possibility of generating the ${}^{3}_{\Lambda_c}\mathrm{H}$ nucleus in the quark-delocalization color-screening model

Siyu Wu,[1,2,3,4] Qian Wu,[2,5,*] Hongxia Huang,[6,†] Xurong Chen,[2,7,‡] Jialun Ping,[6,§] and Qian Wang[1,3,4,‖]

[1]*Key Laboratory of Atomic and Subatomic Structure and Quantum Control (MOE), Institute of Quantum Matter, South China Normal University, Guangzhou, China*

[2]*Institute of Modern Physics, Chinese Academy of Sciences, Lanzhou 730000, China*

[3]*Guangdong Provincial Key Laboratory of Nuclear Science, Institute of Quantum Matter, South China Normal University, Guangzhou 510006, China*

[4]*Guangdong-Hong Kong Joint Laboratory of Quantum Matter, Southern Nuclear Science Computing Center, South China Normal University, Guangzhou 510006, China*

[5]*Department of Physics, Nanjing University, Nanjing 210097, China*

[6]*Department of Physics, Nanjing Normal University, Nanjing 210097, China*

[7]*School of Nuclear Science and Technology, University of Chinese Academy of Sciences, Beijing 100049, China*

(Received 3 August 2023; accepted 6 December 2023; published 2 January 2024)

We probe the existence of the ${}^{3}_{\Lambda_c}\mathrm{H}$ where the $N\Lambda_c$ potentials are derived from the quark-delocalization color-screening model (QDCSM). The $N\Lambda_c$ system is studied and the $N\Lambda_c$ scattering length as well so the effective ranges are obtained in the QDCSM. We construct effective Gaussian-type $N\Lambda_c$ potentials which reproduce the $N\Lambda_c$ scattering data given by the QDCSM. By solving the $NN\Lambda_c$ three-body Schrödinger equation with the Gaussian expansion method, we calculate the energies of the ${}^{3}_{\Lambda_c}\mathrm{H}$ with isospin $I = 0$, $J^P = 1/2^+$ and $I = 0$, $J^P = 3/2^+$ under different color screening parameter μ. The $J^P = 1/2^+$ and $J^P = 3/2^+$ states are both bound when the color screening parameter μ is set to 1.0 fm^{-2} or 1.2 fm^{-2}, where the $J^P = 1/2^+$ state is bound by 0.08–0.85 MeV and the $J^P = 3/2^+$ state is bound by 0.15–1.31 MeV with respect to the deuteron-Λ_c threshold.

DOI: 10.1103/PhysRevC.109.014001

I. INTRODUCTION

The low-energy hadronic system and hadron-hadron interactions are difficult to study due to the nonperturbative nature of quantum chromodynamics (QCD). In order to understand the hadron-hadron interactions and exotic hadronic states, various sophisticated models have been applied. The nucleon-nucleon (NN), hyperon-nucleon (YN), and hyperon-hyperon (YY) interactions have been well constructed by some approaches such as the one-boson-exchange (OBE) model [1–3], chiral effective theory [4], chiral quark model [5–7], and quark-delocalization color-screening model (QDCSM) [8–10]. Recently, the hadron-hadron interactions were extended to the heavy flavor systems. For instance, in Refs. [11,12], the $\Sigma_c\bar{D}$ bound states are found with the chiral quark model. As for the charmonium-nucleon ($c\bar{c} - N$) interactions, since they have no valence quarks in common, the single meson exchange is suppressed and the single gluon exchange is prohibited [13]. Alternatively, the multigluon exchange interactions could be possible as discussed in Refs. [14–17] and the $c\bar{c} - N$ interaction is found to be attractive.

The $\Lambda_c N$ interaction and the possible $\Lambda_c N$ bound state, in which the Λ_c is composed of one up quark, one down quark, and one charm quark, have been studied in several models. With the chiral constituent quark mode, the S-wave $\Lambda_c N$ interaction is investigated in Ref. [18] and they find a $J^P = 2^+$ candidate of the $\pi\Lambda_c N$ three body system. The attractive force between Λ_c and N is also found in Ref. [19] within the the one meson exchange model and the quark cluster model, where a bound $\Lambda_c N$ state with 1 MeV binding energy is obtained. However, the HAL QCD collaboration [20] obtained a weakly attractive S-wave $\Lambda_c N$ interaction based on unphysical quark masses corresponding to pion masses of $m_\pi = 410$–700 MeV and no $\Lambda_c N$ molecular state is confirmed. Recently, an extrapolation of the HAL QCD results to the physical pion mass with the chiral effective filed theory (EFT) [21] was presented [22,23]. It gives that the $\Lambda_c N$ interaction at the physical point is slightly stronger than for that at the large pion masses but still less attractive than the phenomenological predictions for the $\Lambda_c N$ interaction mentioned above [18,19]. As a summary, the existence of the $\Lambda_c N$ bound state is unclear and the theoretical study still remains to be continued [24].

Due to the short lifetime of Λ_c, it is difficult to directly study the $\Lambda_c N$ interaction from the nuclear scattering. Thus, similar to the hypernuclear physics, one can polish the YN and YY interactions from the spectra data of the light hypernuclei instead of the scattering data. For example, in Ref. [25],

*qwu@nju.edu.cn
†hxhuang@njnu.edu.cn
‡xchen@impcas.ac.cn
§jlping@njnu.edu.cn
‖qianwang@m.scnu.edu.cn

the two different YN spin-orbit interactions derived from the quark model and OBE model give different $5/2^+$–$3/2^+$ energy splitting in ${}^{13}_{\Lambda}$C or the $3/2^+$–$1/2^+$ energy splitting in ${}^{9}_{\Lambda}$Be. And the observed values [26–28] may suggest which model of the YN spin-orbit interaction is favored [29,30]. Therefore, in order to further study the $\Lambda_c N$ interaction, it is a natural consideration to extend our research from the hypernuclei to the charmed hypernuclei.

In experiment, the first charmed hypernuclei is claimed to be found in Ref. [31]. The experimental search of the charmed and bottom hypernuclei was also performed at the ARES facility [32]. Several factories including the τ charm factory [33] and the kaon factory (such as the Japan Hadron Facility) may have potential to generate the charmed hypernuclei. In the future, several facilities such as GSI-FAIR, J-PARC [34], or HIAF may be available to check whether the charmed hypernuclei exist or not.

In fact, the theoretical study of the Λ_c hypernuclei dates back to the mid-1970s [24,35–41]. Recently, in Ref. [42], with the one meson exchange model and the quark cluster model, they found a $NN\Lambda_c$ bound state. Soon after that, Garcilazo *et al.* applied the $\Lambda_c N$ interaction derived from the chiral quark model to the $J^P = 3/2^+$ charmed hypertriton and obtained a bound state with binding energy around 0.140–0.715 MeV. Recently, the lattice QCD calculation [20] found that only the A $\geqslant$ 11 charmed hypernculei can be bound with a few MeVs binding energy.

As we know, the forces between atoms (molecular force) are qualitative and similarly between the nucleons. The quark-delocalization color-screening model (QDCSM), which models the molecular force, was developed by Wang *et al.* in 1992 [8] and has been extended to various baryon-baryon interactions and scattering phase shifts [9,10] in the framework of the resonating group method (RGM) [43]. In QDCSM, quarks confined in one baryon are allowed to delocalize to another baryon. The delocalization parameter is determined by the dynamics of the interacting quark system. Besides, the color-screening confinement interaction is used when the two quarks are in different baryons. This gives an extra parameter μ which is normally determined by the mass of the two- body hadron-hadron system.

With QDCSM, co-authored by two of the present authors [44], an attractive $\Lambda_c N$ interaction with a repulsive core was obtained and no $\Lambda_c N$ bound state was found. But no charmed hypertriton was investigated. Thus in this work, we investigate the possibility of the existence of the charmed hypertriton. With the effective $\Lambda_c N$ interaction derived from the QDCSM, we calculate the $NN\Lambda_c$ three-body system. In order to solve the three-body Schrödinger equation, we apply the Gaussian expansion method (GEM) [45].

The paper is organized as follows. In Sec. II, we introduce the effective $\Lambda_c N$ interaction obtained from the QDCSM. The detail of GEM is explained in Sec. III. After explaining the method employed, we show the results and the discussion in Sec. IV. Summary is at the end.

II. QUARK-DELOCALIZATION COLOR-SCREENING MODEL AND $N\Lambda_c$ POTENTIAL

In this section, we introduce the QDCSM and its application in the $\Lambda_c N$ system. In order to describe the $\Lambda_c N$ system, we use the chiral constituent quark model, and the Hamiltonian of the six quarks is

$$H = \sum_{i=1}^{6}\left(m_i + \frac{p_i^2}{2m_i}\right) - T_c + \sum_{i<j}[V^G(r_{ij}) + V^\chi(r_{ij}) + V^C(r_{ij})], \tag{1}$$

where $i\ (j) = 1$–6 is the label of the six quarks composed of the two baryons. The first term means the sum of the masses and kinetic energies of all the quarks. T_c is the kinetic energy of the center of mass. V^C, V^G, and V^χ indicate the confining potential, gluon-exchange potential, and meson-exchange potential, where χ denotes the π, K, or η meson, respectively. The forms of V^G and V^χ are given as follows:

$$V^G(r_{ij}) = \frac{\alpha_{s_{ij}}}{4}\lambda_i\cdot\lambda_j\left[\frac{1}{r_{ij}} - \frac{3}{4m_im_jr_{ij}^3}S_{ij} - \frac{\pi}{2}\left(\frac{1}{m_i^2} + \frac{1}{m_j^2} + \frac{4\sigma_i\cdot\sigma_j}{3m_im_j}\right)\delta(r_{ij})\right],$$
$$V^\chi(r_{ij}) = \frac{\alpha_{ch}}{3}\frac{\Lambda^2}{\Lambda^2 - m_\chi^2}m_\chi\left\{\left[Y(m_\chi r_{ij}) - \frac{\Lambda^3}{m_\chi^3}Y(\Lambda r_{ij})\right]\sigma_i\cdot\sigma_j + \left[H(m_\chi r_{ij}) - \frac{\Lambda^3}{m_\chi^3}H(\Lambda r_{ij})\right]S_{ij}\right\}\mathbf{F}_i\cdot\mathbf{F}_j, \tag{2}$$

where λ_i and F_i are the color Gell-Mann matrices and SU(3) flavor matrices, respectively. The $H(x)$ and $Y(x)$ are the standard Yukawa functions [5]. The S_{ij} is the tensor operator:

$$S_{ij} = \frac{(\sigma_i\cdot\mathbf{r}_{ij})(\sigma_j\cdot\mathbf{r}_{ij})}{r_{ij}^2} - \frac{1}{3}\sigma_i\cdot\sigma_j. \tag{3}$$

For the confining potential, V^C, the color screening confining potential is used when the two quarks are in different baryons:

$$V^C(r_{ij}) = -a_c\lambda_i\cdot\lambda_j[f(r_{ij}) + V_0],$$
$$f(r_{ij}) = \begin{cases} r_{ij}^2 & i,j \text{ are in the same baryon orbit,} \\ \frac{1-e^{-\mu r_{ij}^2}}{\mu} & i,j \text{ are in different baryon orbits.} \end{cases} \tag{4}$$

TABLE I. The channels coupled to the $N\Lambda_c$ states.

States	Channels
$J^P = 0^+$	$N\Lambda_c(^1S_0), N\Sigma_c(^1S_0), N\Sigma_c^*(^5D_0)$
$J^P = 1^+$	$N\Lambda_c(^3S_1), N\Sigma_c(^3S_1), N\Sigma_c^*(^3S_1),$ $N\Lambda_c(^3D_1), N\Sigma_c(^3D_1), N\Sigma_c^*(^3D_1), N\Sigma_c^*(^5D_1)$

It should be noted that, in order to determine the color screening parameter μ (fm^{-2}), we need the total mass of the two baryon system as an input. In the NN system, the parameter $\mu = 1.0$ fm^{-2} is used to fit the deuteron mass or deuteron binding energy. For the $N\Lambda_c$ system, up to now, there is no corresponding experimental measurement to constraint the parameter μ. From the theoretical side, μ is the parameter of the confining potential which is flavor independent. As the result, the value $\mu = 1.0$ fm^{-2} would also work or be at least a benchmark for the $N\Lambda_c$ system. Thus in this work, we vary μ with three different values, 0.8, 1.0, and 1.2 fm^{-2}. The other parameters are determined with a global fitting to the masses of light flavor mesons and charmed baryons Λ_c, Σ_c, and Σ_c^* [44,46].

Normally, the usual quark cluster model gives the single quark wave function as follows:

$$\phi_\alpha(\mathbf{S}_i) = \left(\frac{1}{\pi b^2}\right)^{3/4} e^{-\frac{1}{2b^2}(\mathbf{r}_\alpha - \mathbf{S}_i/2)^2},$$
$$\phi_\beta(-\mathbf{S}_i) = \left(\frac{1}{\pi b^2}\right)^{3/4} e^{-\frac{1}{2b^2}(\mathbf{r}_\beta + \mathbf{S}_i/2)^2}, \quad (5)$$

where $r_{\alpha(\beta)}$ is the coordinate of the single quark to the center of the baryon and S_i is the generating coordinate between the two baryons. In QDCSM, the delocalized quark wave functions are used:

$$\psi_\alpha(\mathbf{S}_i, \epsilon) = (\phi_\alpha(\mathbf{S}_i) + \epsilon\phi_\alpha(-\mathbf{S}_i))/N(\epsilon),$$
$$\psi_\beta(-\mathbf{S}_i, \epsilon) = (\phi_\beta(-\mathbf{S}_i) + \epsilon\phi_\beta(\mathbf{S}_i))/N(\epsilon),$$
$$N(\epsilon) = \sqrt{1 + \epsilon^2 + 2\epsilon e^{-S_i^2/4b^2}}, \quad (6)$$

where $\epsilon(S_i)$ is determined by the dynamics of the quark system.

In Ref. [44], the $J^P = 0^+$ and $J^P = 1^+$ $N\Lambda_c$ scattering phase shifts and the potentials have been studied in QDCSM with the well-developed RGM. The coupled channel effects are considered in the $N\Lambda_c$ system. In total, three/seven channels are included in the $J^P = 0^+/J^P = 1^+$ $N\Lambda_c$ channel (shown in Table I).

In this work, we diagonalize the nondiagonal S matrix and normalize the coupled channel effects into the single channel. We normalize the effects of all three channels into $N\Lambda_c(^1S_0)$ in the $J^P = 0^+$ case. Similarly in the $J^P = 1^+$ state, the effects of all seven channels are normalized into the $N\Lambda_c(^3S_1)$ channel. Thus, the Σ_c (Σ_c^*) and the D-wave components are normalized to the S-wave $N\Lambda_c$ potential.

Then, we construct the effective S-wave $\Lambda_c N$ interactions which reproduce the $\Lambda_c N$ scattering length (a) and the effective range r_0 defined as follows:

$$k\cot\delta = \frac{1}{a} + \frac{1}{2}r_0 k^2 + \ldots, \quad (7)$$

where δ is the scattering phase shift and k is the wave number. Both the scattering length and the effective range are derived within the QDCSM. The values are shown in Table II for three different values, i.e., 0.8, 1.0, and 1.2 fm^{-2}, of μ.

TABLE II. The scattering length and the effective range of $J^P = 0^+$ and $J^P = 1^+$ $N\Lambda_c$ systems. The color screen potential parameter μ is in unit of fm^{-2}.

(J^P, μ)	Scattering length (fm)	Effective range (fm)
0^+, 0.8	−1.57	5.06
0^+, 1.0	−4.88	3.62
0^+, 1.2	−2.58	3.65
1^+, 0.8	−1.92	3.70
1^+, 1.0	−7.11	3.15
1^+, 1.2	−2.88	3.50

As we can tell from the scattering length, the $\mu = 1.0$ fm^{-2} case has the strongest attractive force among the three cases of μ. In order to investigate this, we calculate the scattering length of the $N\Lambda_c$ $J^P = 0^+$ and $J^P = 1^+$ potentials in the single channel case, which means only the $N\Lambda_c(^1S_0)$ and $N\Lambda_c(^3S_1)$ channels are included.

As shown in Table III, all of the potentials in the single channel case are much less attractive than the coupled channel cases. Besides, both $J^P = 0^+$ and $J^P = 1^+$ $N\Lambda_c$ potentials become stronger as the μ grows from 0.8 to 1.2 fm^{-2}. This is reasonable since the μ governs the color screen confining potential which is lower as the μ increases. So it induces the more attractive $N\Lambda_c$ potentials. Then, due to the increase of the μ, the N and Λ_c are closer and thus quarks' spin-spin potential become stronger, which results in the increase of the difference between the $J^P = 0^+$ and the $J^P = 1^+$ potentials. So in Table III, the difference between the $J^P = 0^+$ and $J^P = 1^+$ scattering length (absolute value) grows from 0.06 fm to 0.2 fm as μ increases from 0.8 to 1.2 fm^{-2}.

Therefore, in the QDCSM, the coupled channel effect in the $N\Lambda_c$ potentials is significant. Due to the inclusion of the

TABLE III. The scattering length of the single channel $J^P = 0^+$ and $J^P = 1^+$ $N\Lambda_c$ systems. The color screen potential parameter μ is in unit of fm^{-2}.

(J^P, μ)	Scattering length (fm)
0^+, 0.8	−0.16
0^+, 1.0	−0.53
0^+, 1.2	−1.13
1^+, 0.8	−0.22
1^+, 1.0	−0.68
1^+, 1.2	−1.33

TABLE IV. Fitting parameters of $V_{\rm eff}(r)$ defined in Eq. (8) for the $N\Lambda_c$ effective potentials. The color screen potential parameter μ is in units of fm^{-2}. The V_1 and V_2 are in units of MeV. b_1 and b_2 are in units of fm.

	$^1S_0$			$^3S_1$		
μ	0.8	1.0	1.2	0.8	1.0	1.2
V_1	−115.5	−42.0	−223.5	255.0	−216.4	−226.5
b_1	1.29	1.58	1.20	1.12	1.30	1.20
V_2	160.6	81.3	261.2	292.8	253.3	262.6
b_2	1.05	0.91	1.05	1.01	1.12	1.05

coupled channels, the $N\Lambda_c$ potentials become more attractive and the patterns of their relations with μ are also changed.

The functional form of the effective $N\Lambda_c$ interactions are given by

$$V_{\rm eff}(r) = V_1 e^{-r^2/b_1^2} + V_2 e^{-r^2/b_2^2}. \quad (8)$$

The fitting parameters are listed in Table IV. The obtained effective $\Lambda_c N$ interactions are shown in Figs. 1 and 2, respectively for the $J^P = 0^+$ and $J^P = 1^+$ channel.

As for the NN interaction, we apply the AV8' interaction which is a modified version of the realistic AV18 NN interaction [47]. The tensor force is included in the AV8' interaction and the calculated binding energy of the deuteron is 2.24 MeV.

III. GAUSSIAN EXPANSION METHOD

In order to solve the $NN\Lambda_c$ three-body Schrödinger equation, we apply the Gaussian expansion method and set the three-body wave function as

$$\Psi_{JMTT_z}\left({}^3_{\Lambda_c}\mathrm{H}\right) = \sum_{c=1}^{2}\sum_{s,S,L}\sum_{n_1,l_1}\sum_{n_2,l_2} C_\gamma^{(c)}\mathcal{A} \times \left\{\left[\left(\phi_{n_1l_1}^{(c)}(\boldsymbol{r}_c)\psi_{n_2l_2}^{(c)}(\boldsymbol{R}_c)\right)_L \times \left[\left(\chi_{1/2}^1\chi_{1/2}^2\right)_s\chi_{1/2}^3\right]_S\right\}_{JM}\left(\tau_{1/2}^1\tau_{1/2}^2\right)_{TT_z}\right\}, \quad (9)$$

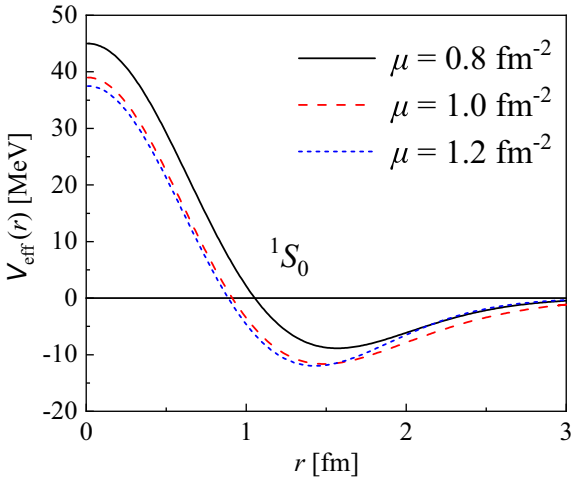

FIG. 1. Effective $N\Lambda_c$ interaction of the $^1S_0$ case.

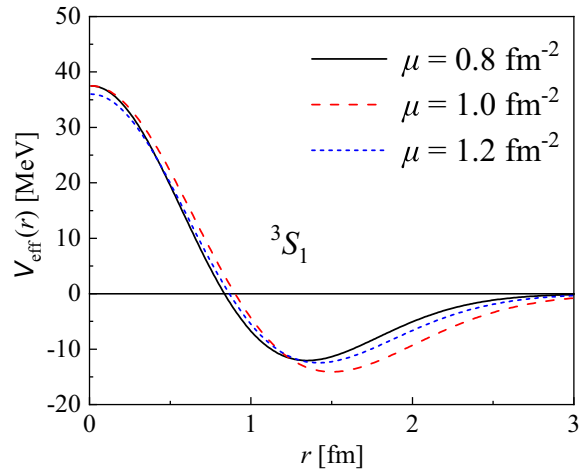

FIG. 2. Effective $N\Lambda_c$ interaction of the $^3S_1$ case.

where the two sets of Jacobian coordinates (labeled as 1 and 2) are shown in Fig. 3. Here, γ denotes $\{L, s, S, n_1, l_1, n_2, l_2\}$. χ and τ represent the spin and isospin wave function of the nucleon or Λ_c, respectively. Note that we omit the isospin wave function of Λ_c since it is an isospin singlet. The $\mathcal{A}$ is the antisymmetric operator between the two nucleons. The relative wave functions between the baryons, corresponding to the two Jacobi coordinates, $\phi_{n_1l_1}(\boldsymbol{r})$, $\psi_{n_2l_2}(\boldsymbol{R})$ are expanded by using the following Gaussian basis functions, applying the GEM:

$$\phi_{n_1l_1}(\boldsymbol{r}) = r^{\ell_1}e^{-(r/r_{n_1})^2}Y_{\ell_1m_1}(\hat{\boldsymbol{r}}),$$
$$\psi_{n_2l_2}(\boldsymbol{R}) = R^{\ell_2}e^{-(R/R_{n_2})^2}Y_{\ell_2m_2}(\hat{\boldsymbol{R}}). \quad (10)$$

The Gaussian variational parameters are chosen to have geometric progression:

$$r_{n_1} = r_{\min}A_1^{n_1-1}, \quad \left(n_1 = 1 - n_1^{\max}\right),$$
$$R_{n_2} = R_{\min}A_2^{n_2-1}, \quad \left(n_2 = 1 - n_2^{\max}\right). \quad (11)$$

Then, the eigenenergies and the coefficients C_γ are obtained by applying the Rayleigh-Ritz variational method.

IV. RESULTS AND DISCUSSIONS

The energy levels of ${}^3_{\Lambda_c}$H with $I = 0$, $J^P = 1/2^+$, and $J^P = 3/2^+$ states are shown in Fig. 4. The binding energies of ${}^3_{\Lambda_c}$H are given with respect to the $N + N + \Lambda_c$ three-body break-up threshold. We calculate the energies of ${}^3_{\Lambda_c}$H without or with the Coulomb force between the Λ_c^+ and the nucleon, which are shown in the left and right columns of Fig. 4. As shown in

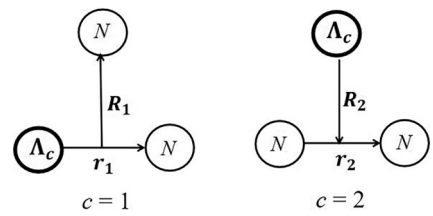

FIG. 3. Jacobi coordinates of the $NN\Lambda_c$ three-body system.

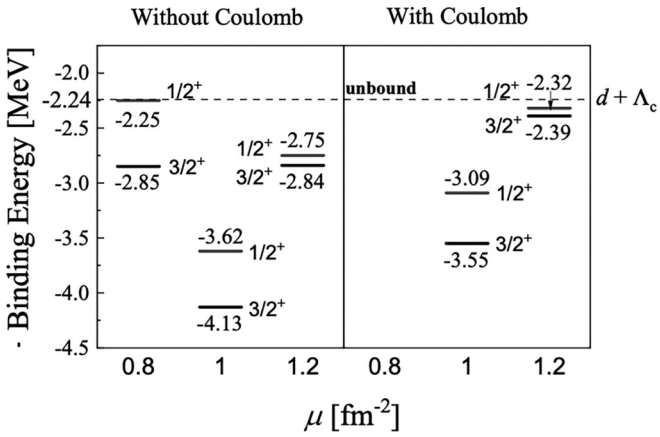

FIG. 4. The calculated energy levels of ${}^{3}_{\Lambda_c}$H. The levels without and with considering the Coulomb force are shown in the left and right figures, respectively, for the color screening parameter $\mu =$ 0.8, 1.0, 1.2 fm^{-2}. The energies are given with respect to the $NN\Lambda_c$ three-body breakup threshold. The $d + \Lambda_c$ threshold is also shown at $E = -2.24$ MeV.

Fig. 4, it is obvious that the binding energies are smaller when we include the repulsive Coulomb force.

The binding energy for the $\mu = 1.0$ fm^{-2} case is larger than the $\mu = 1.2$ fm^{-2} and $\mu = 0.8$ fm^{-2} cases. This can be expected from the $N\Lambda_c$ scattering length in Table. II, in which the $\mu = 1.0$ fm^{-2} case has the largest scattering length for both ${}^1S_0$ and ${}^3S_1$. In the $\mu = 0.8$ fm^{-2} case, no bound state is obtained with the Coulomb force. And when we exclude Coulomb force, a very weakly bound state for the $1/2^+$ state is obtained with the Λ_c separation energy $B_{\Lambda_c} = 0.01$ MeV. As for the $\mu = 1.2$ fm^{-2} case, very weakly bound states with $B_{\Lambda_c} = 0.08$ MeV and 0.15 MeV are obtained, respectively, for the $1/2^+$ and $3/2^+$ states. We find that the energy levels of $J^P = 3/2^+$ state are lower than the $J^P = 1/2^+$ state for all three μ values. To further explore the underlying physics, we compare the S-wave and D-wave components in the final ${}^{3}_{\Lambda_c}H$ and ${}^{3}_{\Lambda}$H (as will be explained later) wave functions in Table V. The S-wave component ($L = 0$ and $S = 1/2$) is also dominant for the $1/2^+$ state which is also around 93% (shown in Table V). Thus, the ${}^1S_0$ $N\Lambda_c$ component is nearly excluded in the $3/2^+$ state while it has a significant contribution in the $1/2^+$ state. On the other hand, since the ${}^3S_1$ $N\Lambda_c$ interaction is more attractive than the ${}^1S_0$ case, the binding energy of the $3/2^+$ state is larger than that the $1/2^+$ state.

Besides, the energy splitting between the $1/2^+$ and $3/2^+$ states does not change significantly when we include the Coulomb force since the Coulomb force does not have a spin-dependent term. The $\mu = 1.2$ fm^{-2} case has the smallest energy splitting which is nearly one order smaller than the $\mu = 0.8$ fm^{-2} and 1.0 fm^{-2} cases. As we discussed in the last paragraph, the much larger $3/2^+$–$1/2^+$ energy splittings for $\mu = 1.0$ fm^{-2} and 0.8 fm^{-2} originate from the larger difference between the ${}^1S_0$ $N\Lambda_c$ potentials and the ${}^3S_1$ $N\Lambda_c$ potentials.

TABLE V. The S-wave and D-wave (in parentheses) components (%) in the ${}^{3}_{\Lambda_c}$H wave functions with $\mu = 1.0$ (fm^{-2}) (second column) and 1.2 (fm^{-2}) (third column). The final column is the S-wave and D-wave components (%) in the ${}^{3}_{\Lambda}$H ($1/2^+$) wave function (see text).

	${}^{3}_{\Lambda_c}$H($\mu = 1.0$)	${}^{3}_{\Lambda_c}$H($\mu = 1.2$)	${}^{3}_{\Lambda}$H
$1/2^+$	93.47(6.53)	93.87(6.13)	94.23(5.77)
$3/2^+$	93.44(6.56)	93.83(6.17)	–

TABLE VI. The Λ_c separation (B_{Λ_c}) energy of ${}^{3}_{\Lambda_c}$H under different models. The units of energy are in MeV. The μ is in unit of fm^{-2}.

	$\mu = 1.0$	$\mu = 1.2$	Ref. [42]	Ref. [48]
$B_{\Lambda_c}(1/2^+)$	0.85	0.08	18.23	–
$B_{\Lambda_c}(3/2^+)$	1.31	0.15	18.89	0.14 –0.75
$1/2^+ - 3/2^+$	0.46	0.07	0.66	–

It is interesting that similar conclusions were made in Refs. [42,48] for the three-body ${}^{3}_{\Lambda_c}$H calculations. As shown in Fig. 9 of Ref. [42], the $J^P = 1^+$ interaction is also stronger than the $J^P = 0^+$ case though their calculated $N\Lambda_c$ interaction is much stronger than ours. For the three-body ${}^{3}_{\Lambda_c}$H calculation, the binding energy of the $J^P = 3/2^+$ state is larger than the $J^P = 1/2^+$ state. In Ref. [48], they also found that the binding energy for the $J^P = 3/2^+$ state in ${}^{3}_{\Lambda_c}$H is larger than the $J^P = 1/2^+$ state. Comparisons of those two works [42,48] are collected in Table VI, where we show the Λ_c separation energies for the $J^P = 1/2^+$ and $J^P = 3/2^+$ states in the $\mu = 1.0$ fm^{-2} and $\mu = 1.2$ fm^{-2} cases, as well as the energy difference between the $1/2^+$ and $3/2^+$. In our calculation, the Λ_c separation energies in the $\mu = 1.2$ fm^{-2} case and the energy of $1/2^+$–$3/2^+$ are smaller than the $\mu = 1.0$ fm^{-2} case. Despite the extremely large binding energies in Ref. [42], the $1/2^+ - 3/2^+$ energy is close to our $\mu = 1.0$ fm^{-2} result. As for the Λ_c separation energies of the $J^P = 3/2^+$ state, our results are consistent with the values in Ref. [48].

As people know [49], the lightest hypernucleus, ${}^{3}_{\Lambda}$H ($J^P = 1/2^+$), is a weakly bound state with the $B_\Lambda = 0.13 \pm 0.05$ MeV while no bound state is found for the ${}^{3}_{\Lambda}$H ($J^P = 3/2^+$) state. In our present calculation, the $3/2^+$ state for ${}^{3}_{\Lambda_c}$H is more bound than the $1/2^+$ state which has an opposite behavior compared with ${}^{3}_{\Lambda}$H. As we mentioned earlier, this is because the ${}^3S_1$ $N\Lambda_c$ potential is more attractive than the ${}^1S_0$ $N\Lambda_c$ potential.

Thus, in order to investigate this opposite behavior in ${}^{3}_{\Lambda}$H, we depict the ${}^1S_0$ and ${}^3S_1$ $N\Lambda$ potentials together with the $\mu = 1.0$ fm^{-2} $N\Lambda_c$ potentials in Fig. 5. The $N\Lambda$ potentials used here are the same as the ones used in Ref. [50] which simulate the G-matrix $N\Lambda$ interaction derived from the Nijmegen model $f(NF)$. As shown in Fig. 5, the ${}^1S_0$ $N\Lambda$ potential is more attractive than the ${}^3S_1$ $N\Lambda$ potential while the opposite relation occurs in the $N\Lambda_c$ potentials. Besides, in the ${}^{3}_{\Lambda}$H ($J^P = 1/2^+$) state, the S-wave component is also dominant (shown in Table V). It should be noted that the calculated B_Λ for the ${}^{3}_{\Lambda}$H ($J^P = 1/2^+$) state is 0.13 MeV which agrees with the experimental data. The NN interaction used in the ${}^{3}_{\Lambda}$H($1/2^+$) is the same as the one used in ${}^{3}_{\Lambda_c}$H

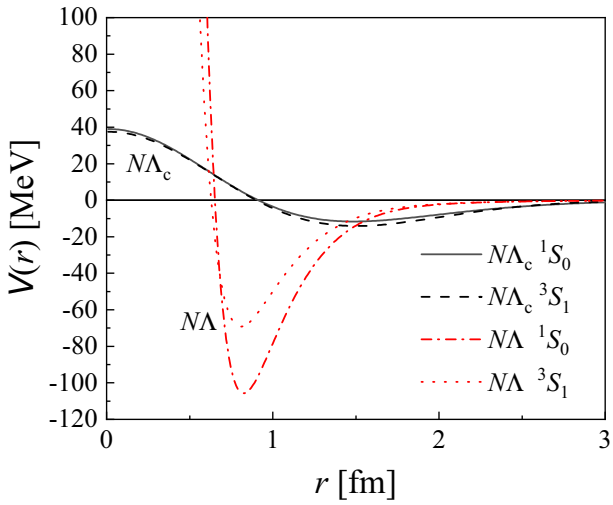

FIG. 5. The $N\Lambda$ $^1S_0$ (red dash-dotted line) and $^3S_1$ (red dotted line) potentials. The $N\Lambda_c$ $^1S_0$ (black solid line) and the $^3S_1$ (black dashed line) potentials in the case of $\mu = 1.0$ fm^{-2} are also shown.

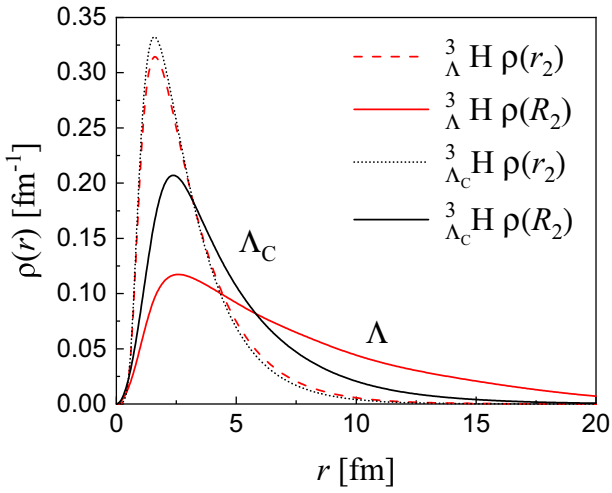

FIG. 6. $\rho(r_2)$ and $\rho(R_2)$ defined in Eq. (12). The black ones are the ${}^3_{\Lambda_c}$H system and the red ones are the hypertriton.

and we also apply the GEM to solve the three-body $NN\Lambda$ system. Therefore, as compared with ${}^3_{\Lambda_c}$H, we think the opposite relations between the $^1S_0$ and $^3S_1$ $N\Lambda$ potentials result in the opposite energy locations of the $1/2^+$ and $3/2^+$ states in the ${}^3_{\Lambda}$H.

Though both the hypertriton and ${}^3_{\Lambda_c}$H$(1/2^+)$ might have small binding energies, the dynamical behaviors between Λ and Λ_c could be different significantly in the nucleus due to the much heavier mass of the Λ_c baryon. In order to investigate this issue, we study the three-body ${}^3_{\Lambda}$H wave functions when calculating the following form:

$$\rho(R_2) = \int \left|\Psi\left({}^3_{\Lambda_c}\mathrm{H}\right)\right|^2 d^3\boldsymbol{r}_2 d^2\hat{\boldsymbol{R}}_2,$$
$$\rho(r_2) = \int \left|\Psi\left({}^3_{\Lambda_c}\mathrm{H}\right)\right|^2 d^3\boldsymbol{R}_2 d^2\hat{\boldsymbol{r}}_2, \qquad (12)$$

where R_2 and r_2 are the Jacobian coordinates with channel $c = 2$, defined in Fig. 3 and $\Psi({}^3_{\Lambda_c}\mathrm{H})$ is the wave function of the ${}^3_{\Lambda_c}$H.

In Fig. 6, we depict the $\rho(r_2)$ and $\rho(R_2)$ of the ${}^3_{\Lambda_c}$H $(1/2^+)$ state in the $\mu = 1.0$ fm^{-2} case. It is obvious that $\rho(r_2)$ reflects the dynamical behavior between the two nucleons and $\rho(R_2)$ reflects the Λ_c's behavior. For comparison, we also show the $\rho(r_2)$ and $\rho(R_2)$ of the hypertriton.

Then, as shown in Fig. 6, we find that the wave function of Λ_c is more compact in the ${}^3_{\Lambda_c}$H $(1/2^+)$ state than Λ in the hypertriton though they have similar binding energies. On the other hand, the nucleon-nucleon wave functions are similar to each other in ${}^3_{\Lambda_c}$H$(1/2^+)$ and the hypertriton. It is well known that in the hypertriton, the Λ wave function is very dilute and is around 10 fm away from the deuteron core. But such behavior may not happen for the Λ_c in the charmed hypertriton according to our calculation.

V. SUMMARY

In this work, we investigate the three-body $NN\Lambda_c$ system within the framework of the quark-delocalization color-screening model and probe the possibility of a bound ${}^3_{\Lambda_c}$H $(T = 0)$.

First, with QDCSM, we normalize the Σ (Σ^*) and the $l = 2$ components into the S-wave $N\Lambda_c$ constituents. We then construct effective Gaussian type $\Lambda_c N$ potentials, reproducing the $\Lambda_c N$ scattering lengths and the effective ranges obtained in the QDCSM for the $^1S_0$ and $^3S_1$ cases. As for the NN interaction, we apply the AV8' realistic NN interaction.

With the above potentials, we solve the three-body problem with GEM and obtain the energy levels of ${}^3_{\Lambda_c}$H $J^P = 1/2^+$ and $J^P = 3/2^+$ states with different color screening parameters μ. We find that both $J^P = 1/2^+$ and $J^P = 3/2^+$ states are bound under the $\mu = 1.0$ fm^{-2} and $\mu = 1.2$ fm^{-2} cases while unbound when $\mu = 0.8$ fm^{-2}. Our calculated binding energy of the $J^P = 3/2^+$ state is consistent with that of Ref. [48]. We also find that the energy difference of $1/2^+$–$3/2^+$ is 70–460 keV and close to another calculation in Ref. [42], i.e., 660 keV.

In our calculation, the energy location of the $3/2^+$ state is lower than the $1/2^+$ state in ${}^3_{\Lambda_c}$H. We find it is because the $^3S_1$ $N\Lambda_c$ potential is more attractive than the $^1S_0$ $N\Lambda_c$ potential within the QDCSM. In contrast, in ${}^3_{\Lambda}$H, the $^3S_1$ $N\Lambda$ potential is less attractive than the $^1S_0$ $N\Lambda$ potential. Thus, only the ${}^3_{\Lambda}$H $(1/2^+)$ state is bound while the $3/2^+$ state is unbound.

At the end, we also compare the dynamical behaviors of Λ_c in ${}^3_{\Lambda_c}$H and Λ in the hypertriton. We find that the Λ_c is closer to the nucleon core than the Λ in the hypertriton due to Λ_c's heavier mass. The experimental search of the charmed hypertriton is urgently needed in order to further study the charmed hypernuclei.

ACKNOWLEDGMENTS

This work is supported by the Strategic Priority Research Program of Chinese Academy of Sciences under Grant

No. XDB34030301, the National Natural Science Foundation of China under Grants No. 12005266, No. 12075288, No. 12375073, No. 11735003, No. 11961141012, and No. 12035007, Guangdong Provincial funding with Grant No. 2019QN01X172, and Guangdong Major Project of Basic and Applied Basic Research No. 2020B0301030008. It is also supported by the Youth Innovation Promotion Association CAS. Q.W. is also supported by the NSFC and the Deutsche Forschungsgemeinschaft (DFG, German Research Foundation) through the funds provided to the Sino-German Collaborative Research Center TRR110 "Symmetries and the Emergence of Structure in QCD" (NSFC Grant No. 12070131001, DFG Project-ID No. 196253076-TRR 110).

[1] R. Machleidt, in *Advances in Nuclear Physics*, Vol. 19, edited by J. W. Negele and E. Vogt (Springer, Boston, MA, 1989).
[2] T. A. Rijken, Phys. Rev. C **73**, 044007 (2006).
[3] T. A. Rijken and Y. Yamamoto, Phys. Rev. C **73**, 044008 (2006).
[4] E. Epelbaum, H. W. Hammer, and Ulf-G. Meissner, Rev. Mod. Phys. **81**, 1773 (2009).
[5] A. Valcarce, H. Garcilazo, F. Fernandez, and P. Gonzalez, Rep. Prog. Phys. **68**, 965 (2005).
[6] Y. Fujiwara, C. Nakamoto, and Y. Suzuki, Phys. Rev. Lett. **76**, 2242 (1996).
[7] Z. Y. Zhang, Y. W. Yu, P. N. Shen, L. R. Dai, A. Faessler, and U. Straub, Nucl. Phys. A **625**, 59 (1997).
[8] F. Wang, G. h. Wu, L. j. Teng, and J. T. Goldman, Phys. Rev. Lett. **69**, 2901 (1992).
[9] J. Ping, H. Pang, F. Wang, and T. Goldman, Phys. Rev. C **65**, 044003 (2002).
[10] J. L. Ping, F. Wang, and J. T. Goldman, Nucl. Phys. A **657**, 95 (1999).
[11] J. J. Wu, R. Molina, E. Oset, and B. S. Zou, Phys. Rev. Lett. **105**, 232001 (2010).
[12] W. L. Wang, F. Huang, Z. Y. Zhang, and B. S. Zou, Phys. Rev. C **84**, 015203 (2011).
[13] A. Yokota, E. Hiyama, and M. Oka, PTEP **2013**, 113D01 (2013).
[14] S. J. Brodsky and G. A. Miller, Phys. Lett. B **412**, 125 (1997).
[15] D. Kharzeev and H. Satz, Phys. Lett. B **334**, 155 (1994).
[16] M. E. Luke, A. V. Manohar, and M. J. Savage, Phys. Lett. B **288**, 355 (1992).
[17] S. J. Brodsky, I. A. Schmidt, and G. F. de Teramond, Phys. Rev. Lett. **64**, 1011 (1990).
[18] A. Gal, H. Garcilazo, A. Valcarce, and T. Fernández-Caramés, Phys. Rev. D **90**, 014019 (2014).
[19] Y. R. Liu and M. Oka, Phys. Rev. D **85**, 014015 (2012).
[20] T. Miyamoto, S. Aoki, T. Doi, S. Gongyo, T. Hatsuda, Y. Ikeda, T. Inoue, T. Iritani, N. Ishii, D. Kawai *et al.* Nucl. Phys. A **971**, 113 (2018).
[21] E. Epelbaum, U. G. Meissner, and W. Gloeckle, Nucl. Phys. A **714**, 535 (2003).
[22] J. Haidenbauer and G. Krein, Eur. Phys. J. A **54**, 199 (2018).
[23] J. Haidenbauer, A. Nogga, and I. Vidaña, Eur. Phys. J. A **56**, 195 (2020).
[24] C. B. Dover and S. H. Kahana, Phys. Rev. Lett. **39**, 1506 (1977).
[25] E. Hiyama, M. Kamimura, T. Motoba, T. Yamada, and Y. Yamamoto, Phys. Rev. Lett. **85**, 270 (2000).
[26] S. Ajimura, H. Hayakawa, T. Kishimoto, H. Kohri, K. Matsuoka, S. Minami, T. Mori, K. Morikubo, E. Saji, A. Sakaguchi *et al.*, Phys. Rev. Lett. **86**, 4255 (2001).
[27] H. Kohri *et al.* (AGS-E929 Collaboration), Phys. Rev. C **65**, 034607 (2002).
[28] H. Akikawa, S. Ajimura, R. E. Chrien, P. M. Eugenio, G. B. Franklin, J. Franz, L. Gang, K. Imai, P. Khaustov, M. May *et al.*, Phys. Rev. Lett. **88**, 082501 (2002).
[29] E. Hiyama and T. Yamada, Prog. Part. Nucl. Phys. **63**, 339 (2009).
[30] O. Hashimoto and H. Tamura, Prog. Part. Nucl. Phys. **57**, 564 (2006).
[31] Y. A. Batusov, S. A. Bunyatov, V. V. Lyukov, V. M. Sidorov, A. A. Tyapkin, and V. A. Yarba, JETP Lett. **33**, 52 (1981).
[32] T. Bressani and F. Iazzi, Nuovo Cimento A **102**, 597 (1989).
[33] S. A. Bunyatov, V. V. Lyukov, N. I. Starkov, and V. A. Tsarev, Nuovo Cimento A **104**, 1361 (1991).
[34] J. Riedl, A. Schafer, and M. Stratmann, Eur. Phys. J. C **52**, 987 (2007).
[35] H. Bandō and M. Bando, Phys. Lett. B **109**, 164 (1982).
[36] H. Bando and S. Nagata, Prog. Theor. Phys. **69**, 557 (1983).
[37] H. Bandō, Prog. Theor. Phys. Suppl. **81**, 197 (1985).
[38] B. F. Gibson, C. B. Dover, G. Bhamathi, and D. R. Lehman, Phys. Rev. C **27**, 2085 (1983).
[39] G. Bhamathi, Phys. Rev. C **24**, 1816 (1981).
[40] K. Tsushima and F. C. Khanna, Phys. Lett. B **552**, 138 (2003).
[41] K. Tsushima and F. C. Khanna, Phys. Rev. C **67**, 015211 (2003).
[42] S. Maeda, M. Oka, A. Yokota, E. Hiyama, and Y. R. Liu, PTEP **2016**, 023D02 (2016).
[43] M. Kamimura, Prog. Theor. Phys. Suppl. **62**, 236 (1977).
[44] H. Huang, J. Ping, and F. Wang, Phys. Rev. C **87**, 034002 (2013).
[45] E. Hiyama, Y. Kino, and M. Kamimura, Prog. Part. Nucl. Phys. **51**, 223 (2003).
[46] M. Chen, H. Huang, J. Ping, and F. Wang, Phys. Rev. C **83**, 015202 (2011).
[47] B. S. Pudliner, V. R. Pandharipande, J. Carlson, S. C. Pieper, and R. B. Wiringa, Phys. Rev. C **56**, 1720 (1997).
[48] H. Garcilazo, A. Valcarce, and T. F. Caramés, Phys. Rev. C **92**, 024006 (2015).
[49] D. H. Davis, Nucl. Phys. A **754**, 3 (2005).
[50] Q. Wu, Y. Funaki, E. Hiyama, and H. Zong, Phys. Rev. C **102**, 054303 (2020).